Fingerprint Sensor Classification via Mélange of Handcrafted Features

Akshay Agarwal Richa Singh Mayank Vatsa
IIIT-Delhi, India
Email: akshaya@iiitd.ac.in, rsingh@iiitd.ac.in, mayank@iiitd.ac.in

***Abstract*—Large scale biometrics projects rely on capturing images/signal from multiple sensors. For example, in India's Aadhaar project, multiple fingerprint sensors of different make and model are used for data collection. Similarly, in law enforcement applications, different agencies use different fingerprint sensors. These scenarios cause two potential problems: (i) sensor inter-operability and (ii) protecting/recording chain of evidence. While sensor inter-operability in fingerprints is a well studied problem, automatically recording chain of evidence is a relatively less explored research problem. For both the problems, one potential approach includes automatically identifying sensors based on the input image. This paper presents a novel fingerprint sensor identification algorithm based on multiple features such as Haralick, entropy, statistical and image quality features. The proposed algorithm is evaluated on a large database with 30,000 images with 15 fingerprint sensor classes. The proposed algorithm achieves an accuracy of 96% and computationally requires less than 10 milliseconds for an image.**

I. Introduction

Prevalence and success of large scale biometrics projects such as UIDAI and FBI AFIS has instigated continuous growth in biometric sensor design and algorithm/system development. Different kinds of sensors are being manufactured and used in these large scale projects to captured the data/images. In such a scenario, the problem of *inter-operability* is common where the images acquired using different sensors are matched together via various pattern matching algorithms. These different sensors, while they capture same biometric modality, may provide different information. For example, as shown in Fig. 1, there are various types of fingerprint sensors such as optical, capacitive, and thermal which can provide *different* information. Looking at these example images, it is very evident that the image quality can vary according to the sensor properties.

In a multi-sensor environment, one important aspect is identifying the sensor from which the image is being captured. This serves two important purposes: (1) helps in establishing the chain of command for forensics and law-enforcement applications and (2) can be useful for addressing sensor inter-operability. In fingerprint recognition, establishing a chain of evidence with tens of devices in the market is an important research challenge. As Bartlow *et al.* [4] have mentioned, we should be able to determine that which image is captured from which sensor, which manufacturer, and which device. Bartlow *et al.* also proposed to utilize sensor noise pattern for identifying the sensor from the fingerprint images and also implemented brand and unit level sensor identification model. Another interesting application of sensor identification can be related to attacks on a biometrics system where biometric templates can be modified [24]. The first step in such cases would be to determine the source model from which the image is generated. It is important to note that very few researchers have worked on identifying biometrics (fingerprint) sensors from the given images.

As mentioned previously, another purpose of sensor identification is related to inter-operability. Several researchers have explored the problem of fingerprint sensor inter-operability, some of them are mentioned in Table I. Ross and Jain [25] studied fingerprint inter-operability with several sensing technologies that are widely used for capturing the fingerprint impressions. They observed that the (i) number of minutia extracted from the images captured using optical sensor is higher than the images captured using solid state sensor and (ii) cross sensor matching performance is lower than the same sensor performance. Ross and Nadgir [26] presented the thin-plate spline model for sensor calibration to improve the cross-sensor performance of the fingerprint matcher. In 2013, Marasco *et al.* [17] showed that the genuine scores are higher when both gallery and probe images are captured using same sensors. They proposed a combination of features and match scores obtained from fingerprint matcher to improve cross-sensor fingerprint recognition performance. Image quality, pattern noise, intensity and direction related features are also proposed to enhance the cross sensor matching performance. Modi *et al.* [20] statistically analyzed the minutia count, image quality, and matching performance. Quality score of the images captured using different sensor shows high similarity

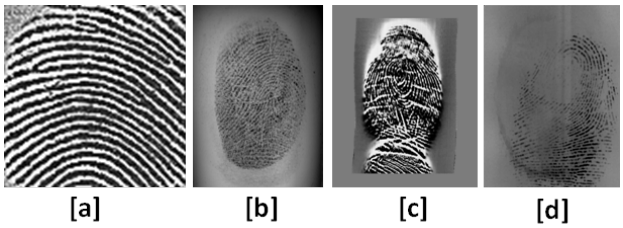

Fig. 1: Samples fingerprint image captured using four different sensors: (a) CrossMatch (Optical), (b) Digital Persona (Optical), (c) Atmel (Thermal-sweeping), and (d) Synthetic. Images are taken from the FVC-2006 [7].

TABLE I: Summarizing the literature in fingerprint sensor inter-operability.

Authors	Database	Contribution
Ross and Jain [25] (2004)	MSU DBI and VERIDICOM	Optical vs Solid state sensors inter-operability case study.
Ross and Nadgir [26] (2008)	MSU	Minutia + Distortion + TPS calibration.
Bartlow *et al.* [4] (2009)	WVU, Clarkson, FVC	Wavelet denoising, PRNU and Correlation noise reference pattern
Modi *et al.* [20] (2009)	Many	Minutia count + Image quality + FNMR.
Jia *et al.* [9] (2012)	Fingerpass	Cross database and sensor type level inter-operability + Verifinger SDK
Lugini *et al.* [14] (2013)	WVU dataset	Large scale study on sensor inter-operability.
Marasco *et al.* [17] (2013)	In-house	Features + Match Score + DET + NFIQ quality.
Mason *et al.* [18] (2014)	In-house	NFIQ and MITRE + COTS.
Yang *et al.* [28] (2015)	Many	Finger vein+ SLIC + ROI + Finger body tracking.

while the minutia count across databases have no relation. *Yang et al.* [28] proposed the super pixel based finger vein ROI extraction across sensors. Mason *et al.* [18] showed fingerprint image quality analysis across sensors and gender using two different quality algorithms. They used NFIQ and MITRE quality algorithms for comparing the performance across images. They used three kinds of matchers to generate the match scores from the gallery and probe images from same and different sensors. The results show that the error obtained with same sensor matching is lower than matching images captured with different sensors. Jia *et al.* [9] prepared the cross device fingerprint database using nine different sensors while considering the model and technology in the consideration. They also observed that the cross-device fingerprint matching gives the higher error in comparison to the same device fingerprint matching. They showed that differences in image resolution and image size can affect the area available for matching. Fingerprint impression can be acquired by pressing or sweeping the finger on the sensor. In this paper, the authors observed large sensor inter-operability between the optical press and capacitive press sensors. Lugini *et al.* [14] performed the large scale fingerprint sensor inter-operability study. They showed that genuine match scores are much higher while matching the same fingerprint images captured using the same sensor. They also observed that false non-match rates are greatly affected by the cross sensor matching while false match rate remains un-affected in sensor inter-operability.

Existing sensor classification techniques can be classified into three groups: i) based on sensor pattern noise [15], [19], ii) using hand-crafted or learned feature extraction and classification [2], [11], and iii) based on color filter analysis [5], [22]. In this paper, we present a fingerprint sensor classification algorithm based on mélange of handcrafted features including texture features, entropy features, image quality, and statistical features. Since several different kinds of variations can be observed with different sensors, the proposed algorithm utilizes a spectrum of features to encode the variations followed by learning a non-linear multi-class classifier for classification.

II. Proposed Fingerprint Sensor Classification Algorithm

Fig. 2 illustrates the steps involved in the proposed algorithm. It uses texture, local intensity, image quality, and statistical features along with a non-linear classification model. Since different sensors provide images of different sizes, they are first resized to a fixed size using the bicubic interpolation. The algorithm extracts four different kinds of features: Haralick [8], entropy, statistical, and image quality measure. Haralick and entropy features are texture features and these are better encoded in the wavelet domain. Therefore, we compute the Redundant Discrete Wavelet Transform (RDWT) of the input fingerprint image. Fig. 3 shows the four bands obtained after the RDWT decomposition. Haralick and entropy features are extracted from these individual sub-bands. Statistical features capture intensity based statistical properties of the image and therefore they are extracted directly from the resized input images only. Similarly, image quality features [3] are extracted from the input images only. The details of feature extraction and classification algorithm are described below.

A. Feature Extraction

Statistical Features: To capture the local intensity variations of the images captured using different kinds of sensors, images are divided into four blocks of equal size. Each block is further divided into four sub-blocks of equal size. For each block and sub-block, mean and standard deviation are calculated. The statistical feature vector is generated by concatenating the mean and standard deviation from each of the sub-blocks and blocks. The total dimension of combined features, F_1, is 40 (32 for the sub-blocks and 8 for the blocks).

Entropy: To calculate the entropy features, each image is first decomposed using two-levels of the redundant discrete wavelet transform. Each level of RDWT decomposition provides four sub-bands, namely approximation, horizontal, vertical, and diagonal. Each sub-band is of equal size as the original image. Entropy over each decomposed sub-bands are calculated using Equation 1.

$$E(H_i) = \frac{\mu_i - \sum H_i(x,y)}{\sigma_i} \tag{1}$$

where $E(\cdot)$ is the entropy of sub-band H_i, and μ_i and σ_i are the mean and standard deviation of the i^{th} sub-band respectively. The entropy of each sub-band is concatenated to generate the second feature vector F_2. The final feature vector is obtained by concatenating all the entropy values measured over each wavelet decomposed sub-band. Computing the features from the second level of RDWT decomposition yields entropy feature vector of size eight values.

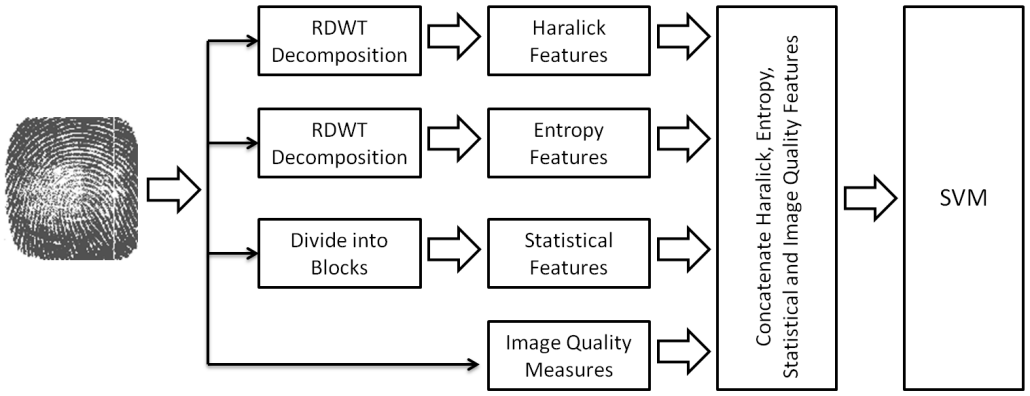

Fig. 2: Illustrating the steps involved in the proposed algorithm for fingerprint sensor classification.

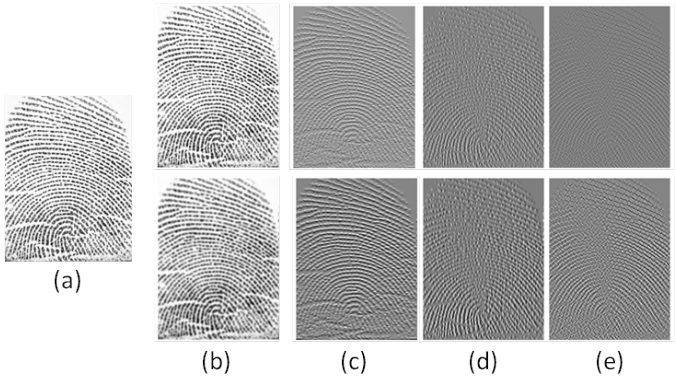

Fig. 3: RDWT decomposition: (a) original image, (b) approximate, (c) horizontal, (d) vertical, and (e) diagonal band. First row represents the first level and the second row contains the second level of RDWT.

TABLE II: Haralick features extracted from the images.

Angular Second Moment	Contrast
Correlation	Sum of Squares: Variance
Inverse Difference Moment	Sum Average
Sum Variance	Sum Entropy
Entropy	Information Measure of Correlation 2
Difference Entropy	Information Measure of Correlation 1
Difference Variance	—

TABLE III: IQM features extracted from the images.

Mean Square Error	Peak Signal to Noise Ratio
Average Difference	Structural Content
Normalized Cross-Correlation	Maximum Difference
Laplacian Mean Squared Error	Normalized Absolute Error
Spectral Magnitude Distortion	Spectral Phase Distortion
Weighted Spectral Distortion	Median Spectral Magnitude Distortion
Median Spectral Phase Distortion	Weighted Median Spectral Distortion
Czekanowski Distance	Mean of Wavelet Sub-bands (4)
Mean of Image	Mean Absolute Error

$$F_{2-1} = \{E(H_{a1}), E(H_{h1}), E(H_{v1}), E(H_{d1})\} \quad (2)$$
$$F_{2-2} = \{E(H_{a2}), E(H_{h2}), E(H_{v2}), E(H_{d2})\}$$
$$F_2 = \{F_{2-1}, F_{2-2}\}$$

Haralick: Texture features are computed with the motivation that fingerprint images are rich in texture which is dependent on how this information is captured by the fingerprint sensor. Hence, encoding *how much* of the texture information is captured using a given sensor can be helpful in identifying the sensor. Haralick texture features [8] measure the intensity homogeneity and other local texture information. To compute the Haralick texture features, images are first decomposed using the RDWT and 13 Haralick features are calculated. The list of Haralick features are mentioned in Table II and the details of these features can be found in [8]. Haralick features are computed over the entire image and each of the RDWT sub-bands thus providing a total of 13 and 104 features, respectively. Thus, the dimensionality of the Haralick feature vector is 117 for an image.

Image Quality Measures (IQM): IQM captures image quality characteristics of the input image [3]. In this research, we have computed 21 image quality measures and these features are listed in Table III. Some of the Image quality measures computed in this paper are explained below:

- Mean of the original image and mean of the single level wavelet decomposed sub-bands are computed.
- Minkowski measures using equation 3 computes the difference between the pixel intensities between the original image and the corrupted image. $\gamma = 1$ corresponds to mean absolute error and $\gamma = 2$ corresponds to mean square error.
- Minkowski Measure

$$M_\gamma = \frac{1}{K}\sum_{k=1}^{K}\frac{1}{N^2}\sum_{i,j=1}^{N}|C_k(i,j) - \hat{C}_k(i,j)| \quad (3)$$

- Correlation Measure

TABLE IV: Summarizing the database characteristics.

Database	Sensors	Sensor Models	Data	Train Data	Test Data
FVC 2002 [16]	4	(a) Identix (Optical) (b) Biometrika (Optical) (c) Precise Biometrics (Capacitive) and (d) SFinGe v2.51 (Synthetic)	3,200	800	2,400
FVC 2006 [7]	4	(a) CrossMatch (Optical) (b) Digital Persona (Optical) (c) Atmel (Thermal-sweeping) and (D) SFinGe v3.0 (Synthetic)	6,720	800	5,920
IIIT-D MOLF [27]	4	(a) Lumidigm Venus IP65 Shell (Optical) (b) Secugen Hamster-IV (Optical) (c) CrossMatch L-Scan Patrol (Optical) and (d) Latent (CMOS sensor)	16,400	800	15,600
CASIA Cross Sensor [1]	3	(a) UrU 4000B (Optical) (b) Authentec AFS-II (Capacitive) and (c) Symwave sw6800 (Capacitive)	3,000	600	2,400

$$M_\gamma = \frac{1}{N^2}\sum_{i,j=0}^{N-1} 1 - \frac{2\sum_{k=1}^{K} min(C_k(i,j), \hat{C}_k(i,j))}{\sum_{k=1}^{K} C_k(i,j) + \hat{C}_k(i,j)} \tag{4}$$

- Spectral Measure

$$\Gamma_k(u,v) = \sum_{m,n=0}^{N-1} C_k(m,n) exp[-2\pi im\frac{u}{M}] exp[-2\pi in\frac{v}{N}] \tag{5}$$

  where $\Gamma_k(u,v)$ denotes the Fourier transform of the original image and $\hat{\Gamma_k}(u,v)$ denotes the Fourier transform of the corrupted image.
- Magnitude spectra (Equation 6) and phase spectra of the image with block and without block are used as a features.

$$M = \frac{1}{KN^2}\sum_{k=1}^{3}\sum_{u,v=0}^{N-1} ||\Gamma_k(u,v)| - |\hat{\Gamma_k}(u,v)||^2 \tag{6}$$

- The weighted sum of the magnitude and phase spectra is also computed.

$$J = \lambda J_M + (1-\lambda) J_\phi \tag{7}$$

  where λ is the weighted factor between the magnitude and phase spectra. J_M and J_ϕ are the Magnitude and Phase spectra respectively. λ is set to 2.5×10^{-5}.

Where k=1..3 represents the color channels and C, $\hat{C}$ are the original and gaussian corrupt image respectively. N is the size of the squared image.

B. Classification

Once the features are extracted, the classification is performed using a multi-class support vector machine [6]. The multi-class classifier is trained according to the number of sensors in the database, i.e. the number of classes is same as a number of sensors. The parameter and kernel of an SVM classifier is learned using training data and it is found that the rbf kernel is performing best for fingerprint sensor classification.

III. Database and Experimental Protocol

The results of the proposed algorithm are shown by combining 4 publicly available databases containing fingerprint images from 15 different sensors. These databases are Fingerprint verification competition (FVC) 2002 and 2006, IIIT-D MOLF, and CASIA multi-sensors database. Table IV summarizes the characteristics of all four databases and Fig. 4 shows sample images from these databases.

- *FVC 2002* [16] is collected using four different sensors. We are using set A of this database for our experiments.
- *FVC 2006* [7] is also acquired from four different fingerprint sensors and we are using Set A of this database.
- *IIIT-D MOLF* database [27] is captured using five different capturing methods. In this paper, we are using data corresponding to four sensors. It contains 16,400 images collected from 100 different subjects.
- *CASIA Cross Sensor* database [1] is collected using three different sensors. 10 fingerprint impressions per person from 100 different fingers are captured for this database.

Combining all four databases, the experiments are performed with $17,960$ images collected from the optical scanner, $2,800$ images from capacitive, $4,400$ images to CMOS, $1,680$ images to thermal sweeping, and $2,480$ synthetically generated images. From each database, 200 images corresponds to particular sensor are used for training the SVM model and the remaining images are used for testing the classifier. As shown in Table IV, out of the total $29,320$ images, $3,000$ images are used for training and the remaining (around 90%) images are used for testing.

IV. Experimental Results and Analysis

Table V shows the classification results of the proposed algorithm and comparison with existing sensor classification techniques [4], [10], [12]. Among these existing algorithms, only Bartlow *et al.* [4] is related to fingerprint sensor identification. The results show that the proposed algorithm yields the classification accuracy of above 96% and is almost 29% higher than the next best performing algorithms. Further, Table V also shows that individual features are at least 4.4% less accurate than the mélange of features. We also observe that if we remove any of the feature set, then the accuracy is reduced. Further, in the proposed algorithm, selection of wavelet decomposition and mother wavelet can have a significant impact on the performance. The proposed algorithm uses RDWT with DB1 mother wavelet. We also performed comparison with RDWT and DWT with two other mother wavelets: DB9 and biorthogonal 9/7. We observed that the classification accuracy

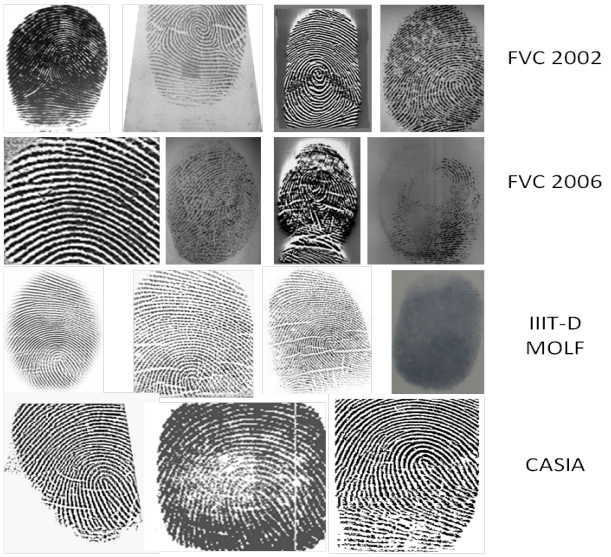

Fig. 4: Sample images from the four database - every image is collected from a different sensor.

TABLE V: Sensor classification results of the proposed and existing algorithms on the multisensor database.

Algorithm	**Classification Accuracy (%)**
HOG [10]	67.18
Li *et al.* [12] (128×128)	34.33
Li *et al.* [12] (256×256)	50.68
Bartlow *et al.* [4]	51.84
Statistical features	90.44
Entropy	52.85
Haralick over image	76.32
Haralick (images + RDWT)	92.08
IQM	90.79
Proposed	**96.52**

with all the combinations varies within 1.5% of each other and RDWT + DB1 yields the best results.

In order to further understand the effectiveness of the proposed algorithm, we manipulated the original images with random gaussian noise, blur, and cropping. The main motivation behind this alteration is that in real time the original image can be affected due to some these variations. We applied two kinds of Gaussian noise, (1) with a variance of 0.01, (2) with a variance of 0.05 and (3) original image is cropped from the center to size 120×120 and Gaussian noise with variance 0.01 is added. Fig. 5 shows sample images with the three artifacts. Table VI summarizes the results of this experiment. Adding noise reduces the accuracy of the proposed algorithm to a certain extent but it has a significant affect on existing algorithms and in the worst case, it reduces the accuracy by almost 25%.

Even though the total dimensionality of all the features is not very high, we performed another set of experiments to understand the effect of feature selection. We implemented six different feature selection algorithms to choose the most important features from the pool of the features proposed.

TABLE VI: Sensor classification accuracy with tampered images (with db1 wavelet filter).

Artifacts	**Proposed**	**HOG [10]**	**Bartlow *et al.* [4]**
Original Images	**96.52**	67.18	51.84
Gaussian Noise (0, 0.01)	**94.57**	71.22	42.87
Gaussian Noise (0, 0.05)	**92.00**	67.96	41.86
Gaussian Noise (0, 0.01) cropping from center	**87.57**	55.38	26.19

The feature selection algorithms used are based on: (1) Mutual Information (MI), (2) Statistical Dependency (SD), (3) Sequential Forward Selection (SFS), (4) Sequential Floating Forward Selection (SFFS) (5) Random Subset Feature Selection (RSFS), and (6) Genetic Algorithm and Information Theory [13], [21], [23]. Statistical feature selection method is based on the criteria that the selected feature have the association with the class label or not. If the feature has high correlation with class labels then it is considered useful for classification. Statistical dependency between two random variables is calculated such that higher the value of SD, the higher the chance of dependence between the feature and its corresponding class label. RSFS is an iterative algorithm that randomly selects a subset of features from the feature pool and performs K-Nearest Neighbor classification to check the relevance of the features. SFS feature selection works in the forward direction of feature set update and the feature set that yields highest accuracy is selected. SFFS works in three steps: the first step is similar to SFS in which some features are selected from the pool and the scores are calculated. In the next two steps, it removes some low relevance features from the selected set based on the principle of conditional exclusion. Least important feature from the selected features is removed and the feature selection algorithm attempts to find the highest scoring features. Finally, for genetic and information theory based feature selection, initial chromosomes are generated by randomly selecting the features with repetition. Based on the maximum relevance and min-redundancy techniques, genetic learning parameters are selected such that the best performing features are preserved. Table VII summarizes the results with a feature selected in terms of a number of features selected as important and the corresponding classification accuracy. A

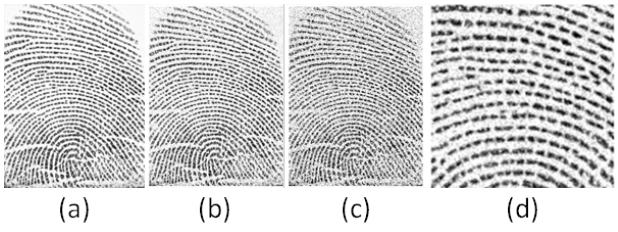

Fig. 5: Images illustrating the effect of adding noise: (a) original images, (b) Gaussian noise of variance 0.01, (c) Gaussian noise of variance 0.05, and (d) Gaussian noise of variance 0.01 after cropping from center to size 120×120.

TABLE VII: Classification accuracy by applying different features selection algorithms on the proposed set of features.

Algorithm	**No. of Features Selected**	**Accuracy %**
Original Features	186	96.52
Mutual Information	100	96.24
Statistical Dependency	100	96.35
SFS	12	91.98
SFFS	19	94.71
RSFS	35	**97.02**
Genetic Algorithm	100	96.83

minimum number of features are given by Sequential forward selection but it also reduces the accuracy to 91.98%. The best results are obtained by random subset feature selection algorithm which selects 35 features and yields an accuracy of 97.02%, slightly higher than original features. Among these 35 selected features, 10 features are statistical features, 10 are Haralick features, 11 are image quality features, and 4 are entropy based features. This shows that all four features are equally important for achieving higher accuracies.

Ideally, sensor classification algorithm should not require a lot of computational resources or time. In that regard, the proposed algorithm is computationally highly cost effective. On an $i7$-4770 desktop PC with 16 GB RAM and Matlab programming, the algorithm requires only 0.008 seconds to process a fingerprint image and provide a classification result.

V. Conclusion

The main contribution of this paper is presenting a novel fingerprint sensor identification algorithm via mélange of multiple features such as Haralick texture, entropy, and intensity information. The algorithm extracts variety of features that are used by a SVM classifier to identify the source of the fingerprint images. The experiments are performed on a combination of multiple databases including FVC 2002, FVC 2006, CASIA cross sensor and IIIT-D MOLF database. The proposed feature extraction algorithm yields an accuracy of over 96% and requires very less processing time which makes it effective for real time applications.

VI. Acknowledgement

This research is supported by Vishveshwarya PhD Fellowship, Government of India.

References

[1] CASIA Cross Sensor Databse. http://biometrics.idealtest.org/index.jsp.

[2] I. Avcibas, S. Bayram, N. Memon, M. Ramkumar, and B. Sankur. A classifier design for detecting image manipulations. In *IEEE International Conference on Image Processing*, volume 4, pages 2645–2648 Vol. 4, Oct 2004.

[3] I. Avcibas, N. Memon, and B. Sankur. Steganalysis using image quality metrics. *IEEE Transactions on Image Processing*, 12(2):221–229, Feb 2003.

[4] N. Bartlow, N. Kalka, B. Cukic, and A. Ross. Identifying sensors from fingerprint images. In *IEEE Computer Society Conference on Computer Vision and Pattern Recognition Workshops*, pages 78–84, June 2009.

[5] S. Bayram, H. Sencar, N. Memon, and I. Avcibas. Source camera identification based on cfa interpolation. In *IEEE International Conference on Image Processing*, volume 3, pages III–69–72, Sept 2005.

[6] C. J. C. Burges. A tutorial on support vector machines for pattern recognition. *Data Min. Knowl. Discov.*, 2(2):121–167, June 1998.

[7] R. Cappelli, M. Ferrara, A. Franco, and D. Maltoni. Fingerprint verification competition 2006. *Biometric Technology Today*, 15(7):7 – 9, 2007.

[8] R. M. Haralick, K. Shanmugam, and I. H. Dinstein. Textural features for image classification. *IEEE Transactions on Systems, Man and Cybernetics*, (6):610–621, 1973.

[9] X. Jia, X. Yang, Y. Zang, N. Zhang, and J. Tian. A cross-device matching fingerprint database from multi-type sensors. In *21st International Conference on Pattern Recognition*, pages 3001–3004, Nov 2012.

[10] O. L. Junior, D. Delgado, V. Goncalves, and U. Nunes. Trainable classifier-fusion schemes: An application to pedestrian detection. In *12th International IEEE Conference on Intelligent Transportation Systems*, Oct 2009.

[11] M. Kharrazi, H. T. Sencar, and N. Memon. Blind source camera identification. In *IEEE International Conference on Image Processing*, volume 1, pages 709–712 Vol. 1, Oct 2004.

[12] R. Li, Y. Guan, and C.-T. Li. Pca-based denoising of sensor pattern noise for source camera identification. In *IEEE China Summit & International Conference on Signal and Information Processing*, pages 436–440, 2014.

[13] O. Ludwig and U. Nunes. Novel maximum-margin training algorithms for supervised neural networks. *IEEE Transactions on Neural Networks*, 21(6):972–984, June 2010.

[14] L. Lugini, E. Marasco, B. Cukic, and I. Gashi. Interoperability in fingerprint recognition: A large-scale empirical study. In *43rd Annual IEEE/IFIP Conference on Dependable Systems and Networks Workshop*, June 2013.

[15] J. Lukas, J. Fridrich, and M. Goljan. Digital camera identification from sensor pattern noise. *IEEE Transactions on Information Forensics and Security*, 1(2):205–214, June 2006.

[16] D. Maio, D. Maltoni, R. Cappelli, J. L. Wayman, and A. K. Jain. Fvc2002: Second fingerprint verification competition. In *16th International Conference on Pattern Recognition*, volume 3, pages 811–814 vol.3, 2002.

[17] E. Marasco, L. Lugini, B. Cukic, and T. Bourlai. Minimizing the impact of low interoperability between optical fingerprints sensors. In *IEEE Sixth International Conference on Biometrics: Theory, Applications and Systems*, pages 1–8, Sept 2013.

[18] S. Mason, I. Gashi, L. Lugini, E. Marasco, and B. Cukic. Interoperability between fingerprint biometric systems: An empirical study. In *44th Annual IEEE/IFIP International Conference on Dependable Systems and Networks*, pages 586–597, June 2014.

[19] M. K. Mihcak, I. Kozintsev, K. Ramchandran, and P. Moulin. Low-complexity image denoising based on statistical modeling of wavelet coefficients. *IEEE Signal Processing Letters*, 6(12):300–303, Dec 1999.

[20] S. K. Modi, S. J. Elliott, and H. Kim. Statistical analysis of fingerprint sensor interoperability performance. In *IEEE 3rd International Conference on Biometrics: Theory, Applications, and Systems*, Sept 2009.

[21] J. Pohjalainen, O. Rsnen, and S. Kadioglu. Feature selection methods and their combinations in high-dimensional classification of speaker likability, intelligibility and personality traits. *Computer Speech & Language*, 29(1):145 – 171, 2015.

[22] A. C. Popescu and H. Farid. Exposing digital forgeries in color filter array interpolated images. *IEEE Transactions on Signal Processing*, 53(10):3948–3959, Oct 2005.

[23] P. Pudil, J. Novoviov, and J. Kittler. Floating search methods in feature selection. *Pattern Recognition Letters*, 15(11):1119 – 1125, 1994.

[24] N. K. Ratha, J. H. Connell, and R. M. Bolle. Enhancing security and privacy in biometrics-based authentication systems. *IBM Systems Journal*, 40(3):614–634, 2001.

[25] A. Ross and A. Jain. Biometric sensor interoperability: A case study in fingerprints. In *Biometric authentication*, pages 134–145. Springer, 2004.

[26] A. Ross and R. Nadgir. A thin-plate spline calibration model for fingerprint sensor interoperability. *IEEE Transactions on Knowledge and Data Engineering*, 20(8):1097–1110, 2008.

[27] A. Sankaran, M. Vatsa, and R. Singh. Multisensor optical and latent fingerprint database. *Access, IEEE*, 3:653–665, 2015.

[28] L. Yang, G. Yang, L. Zhou, and Y. Yin. Superpixel based finger vein roi extraction with sensor interoperability. In *International Conference on Biometrics (ICB)*, pages 444–451, May 2015.